

**Improving Gas-Fired Heat Pump Capacity and Performance
by Adding a Desiccant Dehumidification Subsystem***

Brian K. Parsons
Ahmad A. Pesaran
Desikan Bharathan
Benjamin C. Shelpuk

Solar Energy Research Institute
1617 Cole Boulevard
Golden, Colorado 80401

ABSTRACT

This paper examines the merits of coupling a desiccant dehumidification subsystem to a gas-engine-driven vapor compression air conditioner. A system is identified that uses a rotary, silica gel, parallel-plate dehumidifier. Dehumidifier data and analysis are based on recent tests. The dehumidification subsystem processes the fresh air portion and handles the latent portion of the load. Adding the desiccant subsystem increases the gas-based coefficient of performance 40% and increases the cooling capacity 50%. Increased initial manufacturing costs are estimated at around \$500/ton (\$142/kW) for volume production. This cost level is expected to reduce the total initial cost per ton compared to a system without the desiccant subsystem.

INTRODUCTION

Air-conditioning commercial and residential buildings uses a significant amount of energy. In an effort to decrease cooling costs and reduce energy consumption, the U.S. Department of Energy (DOE) has sponsored research to

The potential for a hybrid system that efficiently handles both latent and sensible cooling loads is great. The system can be used in buildings with high internal moisture generation (such as supermarkets and health clubs) and buildings in humid climates with significant ventilation requirements. The recent high building growth rates in the humid southeastern portion of the United States point toward an ever-increasing potential for such systems.

In this paper, we evaluate the potential of a thermally activated heat pump coupled to a desiccant cooling subsystem. An estimate of the additional capital cost of a promising desiccant subsystem is included.

BACKGROUND

To maintain comfort in buildings during the cooling season, two types of energy building load must be met: sensible load and latent load. The sensible load is characterized by changes in temperature; the latent load is characterized by differences in humidity. Meeting

ternal combustion engines. Using gas as the primary energy source may lead to reduced operating costs compared with conventional electric vapor-compression machines in areas of the United States that have relatively high electric costs.

*This paper was previously presented at the 1989 ASHRAE Winter Annual Meeting (SERI Report No.: TP/254-3402).

The efficiency of a thermally activated heat pump system could be increased if the gas engine waste heat was recovered. This waste heat can be used to regenerate a desiccant dehumidifier that removes moisture from the process air. By combining vapor compression with desiccant dehumidification into a hybrid system, the sensible load can be met by the vapor compression evaporator, which does not have to operate at the low temperatures needed for dehumidification. The latent portion of the load can be met by the desiccant subsystem.

Vapor Compression Systems

The majority of building cooling equipment systems use electric-driven vapor-compression machines. Vapor-compression systems meet sensible loads very effectively. Air passed over the coils of the vapor-compression evaporator gives up heat to the refrigerant; this process chills the air. High heat transfer rates and high-efficiency components make vapor compression attractive for sensible air cooling.

It is less efficient to use vapor-compression equipment to meet latent loads. To remove moisture from the air, the air must be cooled past its dew point; at that temperature the water condenses on the coils. In some systems, the air is now colder than the required delivery temperature dictated by comfort and the sensible load. Depending on the cycle and system configuration, additional energy may be needed to reheat the air to the delivery temperature. These processes are illustrated in Figure 1. In

most vapor-compression systems, the evaporator coil must operate 40° to 60°F (5° to 15°C) cooler than the delivery temperature in order to chill the air to its dew point. The coefficient of performance (COP), defined as cooling output divided by energy input, of the vapor-compression machine is lowered by around 10% to 20% as a result (Howe 1983; Schlepp and Shultz 1984).

Desiccant Cooling Systems

Desiccant systems are well suited to reduce latent loads. The process air is brought in contact with a material with a high affinity for water. Moisture is adsorbed or absorbed by the desiccant material. During this process the heat of adsorption or absorption is released in the desiccant, resulting in higher air temperature. To meet sensible loads, stand-alone desiccant systems over-dry, then evaporatively cool the air to the desired supply temperature (see Figure 2). Since the dehumidification process results in dryer and warmer supply air, the process may be considered a way to convert latent loads into sensible loads.

The desiccant requires regeneration (drying) to remove the moisture picked up from the process air. A hot, regeneration airstream is passed over the moisture-laden desiccant. The regeneration air can be heated by solar collectors, electric heaters, gas burners, or waste heat sources.

Hybrid Cooling Systems

Combining components of a vapor-compression system with a desiccant system results in a hybrid that can efficiently meet the sensible and latent cooling loads. The vapor-compression machine in a hybrid system operates with higher evaporator temperatures, resulting in a higher thermal COP than vapor-compression-alone units. In addition, the hybrid system requires no reheat. The dehumidifier must only remove the moisture to meet the latent load since the sensible load is met by the vapor-compression machine; no overdrying is required (see Figure 3). This process reduces the size of the dehumidifier and the amount of energy required to regenerate the dehumidifier compared with a stand-alone desiccant system.

Another advantage of the hybrid system is it reduces the required energy input (increased overall COP). Heat rejected by some components may be used to regenerate the desiccant, which eliminates or reduces the need for external regenerative heat. Hybrid systems have the option of using the heat rejected by the vapor-compression condenser for regeneration. If a gas engine is used to drive the compression (instead of the usual electric motor), significant amounts of engine waste heat may be available.

DESICCANT MATERIALS AND DEHUMIDIFIER GEOMETRY

Several different hybrid systems have been installed in specialized applications with unique cooling requirements (Meckler 1986). In each of these cases, as well as studies examining the analytical, experimental, and beginning commercialization of desiccant cooling-only systems (Crum 1986; Meckler 1987; Jurinak 1982; Turner et al. 1987), the dehumidifier component performance has the greatest effect on overall system performance. Dehumidifiers have not yet been produced in volume. Some think that the desiccant dehumidifier has room for cost reduction and performance improvements.

The performance of a desiccant dehumidifier depends mainly on the type of desiccant material used, the internal geometry of the dehumidifier (i.e., how the desiccant is deployed within the dehumidifier matrix), and the operating parameters.

The material type affects size, range of operation (temperature, humidity), efficiency, cost, and service life of a dehumidifier. The desiccant choice also affects the thermal COP and cooling capacity of a system. The geometry of a dehumidifier affects its pressure drop, size, and cost and, thus, the thermal and electrical COPs and cost of a cooling system. Control strategies can also affect the overall performance. The optimum combination of desiccants and geometries can provide high-efficiency and low-cost dehumidifiers for air-conditioning applications.

In this study, after an initial screening we selected three materials for detailed analysis: silica gel, lithium chloride, and molecular sieve. Silica gel has a high moisture recycling capacity and was identified by several investigators (e.g., Jurinak 1982) as being the most attractive available commercial solid desiccant. Lithium chloride (a hygroscopic salt) is used in currently available commercial dehumidifiers and is considered one of the state-of-the-art desiccants for wheel-type dehumidifiers. Molecular sieves have been recommended (Kinast et al. 1982) for gas-fired applications because of physical stability, resistance to fouling, and high moisture cycling capacity at high regeneration temperatures (248° to 428°F [120° to 220°C]).

We have completed considerable research on advanced dehumidifier geometries (e.g., Bharathan et al. 1987a, b; Maclaine-cross and Parsons 1986). For this study we selected a parallel-passage, rotary dehumidifier for detailed analysis (Figure 4). Parallel-passage geometries have high rates of heat and mass transfer and low pressure drop. A typical measure of heat transfer to pressure drop ratio, the Stanton number divided by the friction factor (St/f), is typically 0.49 for parallel passages compared with 0.06 for packed beds. A rotary dehumidifier was chosen over two-bed configurations for ease of control and constant outlet conditions.

The same basic wheel design as previously described was used for evaluating desiccant materials. Based on experience from experiments discussed in Bharathan et al. (1987), for typical small to medium cooling loads and a desired pressure loss of around 0.5 to 0.6 in of water (130 to 150 Pa), we arrived at a wheel outside diameter of 3.3 ft (1.0 m) and a wheel depth of 4 in (0.1 m). A design flow rate of 1120 cfm (0.6 kg/s) was used for both the process and regeneration streams for the dehumidifier. The wheel was divided equally into regeneration and process volumes. The maximum number of transfer units is achieved with the minimum practicable passage size. A matrix with a center-to-center spacing of 31 mil (0.8 mm) for the substrate sheets is practicable with current wheel manufacturing techniques. The wheel has 16 support spokes, which is prototypical of existing commercial rotary heat exchangers (PTY 1984).

For the design of the solid particle wheel (silica gel and molecular sieve), microbead particles were used with a size range of 3 to 4 mil (75 to 105 μm). The substrate is 0.4 mil (10 μm) thick polyester tape coated on both sides with 0.4 mil (10 μm) of adhesive. The resulting nominal air passage gap is 23 mil (0.580 mm). Blockage of the nominal frontal area is 27.5%, and the actual flow area for each air passage (process and regeneration) is 2.94 ft² (0.273 m²). About 22 lb (10 kg) of desiccant were used, and the weight ratio of desiccant to total wheel weight was 0.78.

The hygroscopic-salt desiccant wheel design is similar to that of the solid particle wheel except that instead of a thin tape with particles attached by adhesive, a porous fiberglass matrix impregnated with the salt is used. We set the thickness of the matrix equal to 8.7 mil (0.22 mm) so the blockage and design pressure drop would be equal for solid and hygroscopic salt desiccant wheels. To prevent the salt solution from dripping from the matrix, the matrix should be impregnated with a salt and water solution in equilibrium with air at the worst possible operating condition. For this condition we selected a temperature of 95°F (35°C) and 95% relative humidity. This results in a water-desiccant ratio of 16.6 lb H₂O/lb LiCl. For the matrix we used 18 lb (8.2 kg) of fiberglass to hold 2.4 lb (1.1 kg) of lithium chloride and a desiccant fraction of 0.116.

Dehumidifier performance was determined using the detailed analogy method (combined potential and specific capacity ratio). This method allows the coupled, simultaneous, partial differential governing equations to transform into independent equations. The key features of the equations are retained, and properties of different desiccants are easily integrated, yet solutions are much quicker than finite difference methods. Detailed descriptions of the model are beyond the scope of this paper but can

be found in Parsons et al. (1987), Bharathan et al. (1987a, b), and Maclaine-cross (1978).

For a silica gel rotary dehumidifier test article (Bharathan et al. 1987a, b), predicted effectiveness of exchange using the analogy method was confirmed to lie within $\pm 10\%$ of the experimentally measured values. The proposed dehumidifier design for the present application is similar to the tested configurations, and thus the predicted performance is expected to be well within acceptable engineering uncertainty limits for a silica gel parallel-passage dehumidifier. The method was extended to molecular sieve and lithium chloride wheels but predictions have not been verified through actual experiments.

Comparison of Three Desiccant Materials Performance

Comparisons of outlet process and regeneration air states for the three materials selected (microbead silica gel, lithium chloride, and molecular sieve) were performed for a variety of conditions. Although the exhaust portion of the thermally activated heat pump (TAHP) waste heat is available at high temperature, we found that the amount of waste heat available, at typical latent load fractions, and commonly desired cooling delivery temperatures result in regeneration temperatures in the same range as found in solar desiccant systems (167° to 194°F [75° to 90°C]). Figure 5 shows the outlet air states for the three wheel materials with flow rates of 1120 cfm (0.6 kg/s) for both airstreams. Inlet airstream humidities of 0.015 lb water/lb dry air were used and the process and regeneration airstream inlet temperature was set at 95°F (35°C) and 184°F (85°C), respectively. The various outlet states are obtained by varying the dehumidifier wheel rotational speed. There is a minimum outlet process air humidity at a certain rotational speed that corresponds to the maximum outlet regeneration air humidity.

The microbead silica gel wheel produces the lowest outlet humidity, but the difference between the silica gel and lithium chloride wheel is not large. At the lowest humidity point, the silica gel wheel produces an outlet condition of 154°F (68°C) and 0.0057 lb water/lb air, and the lithium chloride wheel produces an outlet of 147°F (64°C) and 0.0061 lb/lb. The molecular sieve wheel does not remove as much water vapor from the process air as the other materials since it requires higher regeneration temperatures. It may be possible to take advantage of the portion of heat available at high regeneration temperature with a wheel using several desiccant materials, but this possibility was not examined.

We selected the microbead silica gel wheel as the baseline wheel for systems evaluation. Process air humidities were lowest using silica gel and the practical problems of lithium chloride dripping out of the matrix are avoided.

System Configurations

Many component arrangements are possible for conventional desiccant systems (Crum 1986; Kettleborough et al. 1986; Meckler 1986) and hybrid systems (Howe 1983; Schlepp and Schultz 1984; Domingo 1986). Most hybrid systems begin with two airstreams similar to conventional desiccant systems. The process airstream, which is delivered to the space to meet the load, typically is first passed through a dehumidifier where it is dried and warmed. Most hybrid system configurations pass the process air through the vapor compression heat pump (evaporator) immediately before the air is delivered to the space. The main difference between the process stream of previously examined hybrid systems is the arrangement of components between the dehumidifier and vapor compression evaporator. Possibilities include heat exchangers and direct and indirect evaporative coolers. The regeneration stream, used to remove the moisture from the dehumidifier, is typically heated by a series of components that might include the vapor compression condenser, a regenerative heat exchanger, waste heat recovery, and auxiliary heat sources.

The first system configuration examined here and a representative psychrometric chart of the air processes are shown in Figure 6. In this layout, only the flow required to meet the fresh air requirement is passed through the dehumidifier. The cooled, dehumidified fresh air (point 3) and the remainder of the process air (point 6) are passed through the vapor compression system for sensible cooling only. In the dehumidification regeneration stream, a sensible heat exchanger coupled to the supply stream is used instead of recovering heat from the vapor compression condenser. Temperatures at the exit of the first regeneration heating step (point 8) would be limited to around 140°F (60°C) if the condenser was used, and using the heat exchanger results in higher temperatures of around 158°F (70°C). Additional regenerative stream heating is then provided by waste heat from the gas engine.

Figure 7 shows a schematic of the second system considered here and a representation of the component operations on a psychrometric chart. After being dried (point 2), the process air is cooled in either an indirect evaporative cooler or an ambient heat exchanger to point 3. The vapor compression evaporator supplies the remaining required sensible cooling to the process stream. Heat from the vapor compression condenser is recovered for regeneration of the desiccant, followed by waste heat recovery from the internal combustion engine water jacket and exhaust. This system configuration results in a larger dehumidifier than the first configuration since all the room-delivered air is dried.

Any additional heat required to bring the regeneration stream up to the regeneration temperature is provided by an auxiliary source, assumed to be an indirect natural gas burner with an efficiency of 90%.

System Modeling

The indirect evaporative cooler, direct evaporative cooler, and sensible heat exchangers are all modeled as constant effectiveness devices. The gas-fired internal combustion engine was modeled after equations presented by Segaser (1977). By using a load fraction (defined as actual load/full capacity) of 0.9, the engine efficiency is 33%, water jacket waste heat is 23% at 212°F (100°C), and exhaust gas waste heat is 27% at 1148°F (620°C). The exhaust gas heat recovery is limited by condensation of corrosive combustion products at around 350°F (175°C). It was judged that the remaining waste heat (lube oil, radiation, etc., making up the remaining 17%) was not economical to recover.

Heat pump performance is modeled as presented by Howe (1983). Note the systems configurations limit the vapor compression load to sensible cooling only. The COP is calculated from a curve fit using nonlinear regression techniques from data for commercial 20- to 70-ton units (Howe 1983). Nonstandard operating conditions were accounted for by using data from a commercial heat pump (Howe 1983). The equation for COP is

$$\text{COP} = 3.68 + 0.162 \text{ FLR tons exp } (-0.183 \text{ FLR tons}) - 0.753 \text{ FLR} - 0.073 \text{ tons} - 0.03998 (T_{\text{cond,in}} - T_{\text{evap,in}} - 15) \quad (1)$$

where FLR is the fractional load ratio (load/full capacity) set to 0.90. In this study, tons are the load in those units. The term $T_{\text{cond,in}}$ is the condenser air inlet temperature, and $T_{\text{evap,in}}^*$ is the evaporator air inlet saturation temperature.

In this paper, performance is evaluated at the American Refrigeration Institute (ARI) standard design point; 75°F (35°C) and 0.0142 lb/lb humidity ratio for ambient, and 80°F (27°C) and 0.0111 lb/lb humidity ratio for the room. Although performance must be evaluated at numerous states and compared with load profiles for a given location for a complete evaluation of the system, comparison at these conditions gives an indication of relative merits. The ARI room state is slightly outside (<2°F [1°C]) the ASHRAE comfort zone defined by Standard 55-74. We feel use of the ARI standard is appropriate for design point comparisons because the ARI ambient condition is quite harsh. Use of the ASHRAE comfort zone would be appropriate for off-design or seasonal performance evaluations. Yearly performance values are significantly higher than performance at the ARI design point for many U.S. cities (Warren 1985).

The building cooling load calculations are used to find the supply airflow rate, temperature, and humidity. For the system results presented in this study, an example cooling load of 10.5 tons (37 kW) was used. This value includes cooling loads from internal loads and transfer through the building perimeter. It does not

include the load imposed on the machine by the fresh air requirement. A fresh air requirement of 112 cfm/ton (15 L/kJ) of cooling was used in this study, 1190 cfm (0.56 m³/s). This value is representative of many buildings, but higher ventilation rates may be required for energy-efficient construction or specialized applications. Using this fresh air requirement implies a partial recirculation mode of operation. These loads resulted in a 3.3 ft (1 m) diameter wheel for the first system configuration.

Combining the building and ventilation loads using the described ARI design point results in a total load on the hardware of 12.5 tons (46 kW), of which 30% is latent capacity.

A final assumption of the load calculations is that the enthalpy difference between the room and supply air is limited to 6.45 Btu/lb (15 kJ/kg) for comfort. This limitation resulted in a room air delivery state of the 62°F (16.5°C) and 0.0097 lb/lb absolute humidity. The total room air flow rate for these loads is 4450 cfm (2.47 kg/s) (1000 cfm [0.56 kg/s] fresh air).

PERFORMANCE RESULTS

The two TAHP-desiccant hybrid systems were compared using component efficiencies and pressure drops summarized in Table 1. In addition, fan efficiency was assumed to be 50%. These values correspond to relatively conservative existing commercial equipment.

Table 2 summarizes load characteristics and Table 3 summarizes the performance of the two hybrid systems using these commercial components. A total equivalent thermal COP is used and defined as

$$\frac{\text{total cooling capacity}}{\text{gas input} + \text{electric input}/0.3} \quad (2)$$

The factor of 0.3 is based on a conversion efficiency from fuel to electricity of 30%. For a complete evaluation, relative electricity and gas cost factors should be included to arrive at an overall COP. These factors vary widely across the country, so a generic factor was used for relative comparison of systems in this paper.

System 1

The regeneration temperature of 185°F (85°C) was chosen to minimize auxiliary energy and to achieve high overall COP.

Note that the dehumidifier inlet state is not identical to the conditions used in the wheel comparisons of Figure 5. Because we are using the ARI design point, the outlet state is slightly different.

Adding on the desiccant dehumidification subsystem (including the dehumidifier, heat exchangers, evaporative cooling, and additional fans) to the vapor compression unit increases the performance of the total system in several

ways. First, the temperature and humidity of the air entering the vapor compression evaporator in the hybrid system is different than if a vapor compressor was meeting the total cooling load. The COP of the vapor compression unit is dependent on the state of the entering air (see modeling discussion). If the same fresh and recirculation airflows were used in a vapor compression system alone, the entering wet-bulb temperature would have been 70°F (21°C) and the resulting vapor compression COP (defined as cooling/compressor work) would have been 3.07. The hybrid system evaporator wet-bulb for the conditions presented in Table 2 is 66°F (19°C) and the vapor compression COP is 3.18. This higher COP results in a decrease in the amount of fuel required to meet a given load.

Second, since the vapor compression subsystem does not handle any dehumidification load, process air does not need to be reheated. The reheat energy for the above load, had it been met by vapor compression alone, would have been approximately 24,400 Btu/h (7.2 kW), which could be provided by a number of sources including heat waste.

The most important advantage of adding the dehumidification subsystem is the added cooling capacity. The desiccant subsystem adds 4.4 tons (15.5 kW) of cooling capacity when using the engine waste heat. These conditions require only a small amount of supplementary gas heat (4400 Btu/h [1.3 kW] compared with 1.0 × 10⁶ Btu/h [30.9 kW] to run the gas engine) to regenerate the desiccant. If we consider the waste heat as a free heat source, the energy input to obtain this increased capacity is only 4400 Btu/h (1.3 kW) in this example. A gas COP of the desiccant subsystem computed on this somewhat artificial basis is near 12. At other conditions, this add-on COP can be infinite since no additional auxiliary gas is needed; all regeneration heat is supplied by the waste heat from the engine.

A gas-engine-driven cooling system operating with vapor compression only and under conditions comparable to the hybrid system presented in Table 2 has an overall gas COP of 1.01 (when reheat is not included since reheat could be taken from any number of "free" heat sources). Using the desiccant dehumidifier subsystem increases the gas COP by more than 40% to 1.42.

System 2

In the second system configuration, all the process air passes through the dehumidifier subsystem components and the vapor compression evaporator.

Room air was mixed with the minimum required fresh air as the source of the supply air to minimize the required capacity, and the ambient mixed with the remaining room air as the source of the regeneration stream. Both air process paths used a flow rate of 4450 cfm (2.47 kg/s).

Results for a regeneration temperature of 122°F (50°C) are presented. Higher regeneration temperatures resulted in increasing auxiliary regeneration energy requirements, and lower regeneration temperatures resulted in excess waste heat being available.

Note that the electric COP is not broken down into vapor compression and desiccant subsystem contributions since in this system the two subsystems have the same airflow paths.

System Selection

The System 2 design is quite different from the System 1 design. The gas COP for System 2 is somewhat higher, but since all the process air passes through the dehumidifier and other desiccant subsystem components, the electric COP decreased by around 40%. Combined equivalent COP is slightly greater for System 1. Although these performance parameters are important, perhaps the largest difference between the two systems is the component size. The vapor compression/engine capacity is around 25% lower for System 2 since the desiccant subsystem handles more of the sensible load through the evaporative coolers. The desiccant subsystem components for System 2 are around 4.5 times larger than those used in System 1 because the full supply airflow passes through them. Larger airflow rates result in a dehumidifier diameter of greater than 6.6 ft (2 m) for System 2, and the dehumidifier for System 1 is 3.3 ft (1 m) in diameter. The probable increase in cost for System 2 over System 1 is perhaps not warranted by the increase in performance. Therefore, we chose System 1 as the better of the two systems.

System Layout and Cost

The chosen system was laid out and the manufacturing cost estimated to evaluate the economics of the performance improvement.

The physical integration of a desiccant dehumidifier subsystem and thermally activated heat pump components can be accomplished with stand-alone units for the two subsystems, as shown in Figure 8.

In the previous analysis, hot exhaust gas is delivered directly to the desiccant subsystem to achieve the final temperature boost in the dehumidifier regeneration airstream. An alternative (assumed in the costing and layouts of this section), which is more practical and easily integrated into the system, uses an exhaust gas-to-cooling water heat exchanger. The engine cooling water delivered to the desiccant subsystem, therefore, operates at boosted temperature. The performance of this modified system is nearly equivalent to the System 1 layout.

Several assumptions of the design and cost presented in this section are

- o The cost of the desiccant subsystem regeneration air heater probably should be credited against the cost of the internal combustion engine cooling radiator. This credit was not included in our cost estimate.
- o We did not account for the effect of the increased back pressure in the exhaust system on engine performance.
- o Integration of the two subsystems allows an increase in the vapor compression evaporator refrigerant pressure and temperature, which results in an increase in the heat pump COP, which is reflected in the increased overall system COP. There may also be a change in cooling capacity at higher evaporator temperature that would require resizing the coil. However, we assumed that the cooling capacity is the same.

The dehumidification subsystem can be contained within an envelope 3.3 by 3.3 by 5.9 ft (1 by 1 by 1.8 m) and has the operating specifications shown in Table 4.

Table 5 provides a summary of the cost breakdown for the system described as a nominal 4.4 ton (15.5 kW) capacity. The cost estimates presented in this section come from Maclaine-cross (1986) and Maclaine-cross and Parsons (1986) plus current quotes from manufacturers. These sources are recent, and all presented costs can be assumed to be 1987 dollars for volume production. Volume production of 10,000 units/yr is essential to bring dehumidifier costs to the estimated levels. The conclusion is that the manufacturing first cost of a desiccant cooling add-on to an internal-combustion-engine-driven vapor compression system would be near \$490/ton (\$140/kW) in the sizes described in this paper, using current state-of-the-art technology. This represents a realistic cost goal, and there is opportunity for performance gain in achieving higher effectiveness for heat and mass transfer systems (dehumidifier, heat exchangers, and evaporative cooler).

The desiccant cooling dehumidification subsystem described in this report is assembled using components that are, for the most part, conventional in heating, ventilation, and air-conditioning equipment. The single exception is the desiccant bed that corresponds to the design used in recent experimental prototype units (Bharathan et al. 1987a). A desiccant dehumidifier having nearly the same performance using lithium chloride solution impregnated into a porous matrix is commercially available. In general, the performance of the dehumidifier and the other heat exchangers can be improved by increasing their effectiveness. This can be done by decreasing air velocity and increasing flow length in the components. This, however, increases the size, cost, and air pressure drop. A complete economic and performance trade-off study is required to fully resolve these issues.

If we assume that the cost estimates for the conventional equipment are within 10% (applicable to general engineering estimates) and the cost of the silica gel dehumidifier is within $\pm 50\%$, the overall subsystem cost estimate has an uncertainty of 18% since the dehumidifier cost is only 20% of the total desiccant subsystem manufacturer first cost.

CONCLUSIONS AND RECOMMENDATIONS

The performance of a TAHP system can be greatly improved by adding a desiccant cooling subsystem. Specifically, for the selected system layout at ARI standard design conditions:

1. The gas COP is increased by 40%.
2. The total cooling capacity is increased by approximately 50%.

The selected hybrid system that separately handles latent and cooling load can be designed as a stand-alone add-on package with simple, standard system interfaces. For a unit that adds about 4.4 tons of cooling capacity to a 10.5-ton TAHP, components can be integrated in a 3.3 by 3.3 by 5.9 ft (1 by 1 by 1.8 m) package.

We estimate the first manufacturing cost of the System 1 configuration add-on desiccant subsystem package to be \$2150 or about \$490/ton of additional cooling capacity for volume production. Current TAHP system first costs are about \$1500/ton (Domingo 1986), which includes manufacturer, distributor, and retail profit but not installation. Maclaine-cross and Parsons (1986) indicate a cost factor of approximately two should be applied to the \$490/ton figure to find a retail cost. Therefore, it is likely that adding a desiccant subsystem may decrease the retail first cost per unit of cooling delivered and increase the gas COP by 40% (fuel consumption is around 60% of a heat-pump-only system). Operating cost advantages of the proposed hybrid system depend on local electric and gas rate structures. Relative comparisons in this study were made using a rough 0.3 gas-to-electric conversion factor.

Use of silica gel resulted in the highest moisture removal effectiveness of the three materials examined at regeneration temperatures of 203°F (95°C) or less. Predictions using lithium chloride resulted in only 5% less moisture removal. Molecular sieve dehumidifier performance predictions indicated 35% less moisture removal than silica gel; thus, this material is not as suitable for these regeneration temperatures. Higher regeneration temperatures using molecular sieves raise the dehumidifier and process air temperature. Thermal COP decreases because of the increased cooling load provided by other components. Therefore, the molecular sieve is not appropriate for this system application.

It is possible to regenerate the desiccant dehumidifier with fairly low regeneration temperatures and meet cooling loads with typical latent heat to sensible heat ratios with very little auxiliary added heat. The quantity of waste heat available and the desire to minimize auxiliary input resulted in regeneration temperatures of 122° to 185°F (50° to 85°C) being used with these wheels and system layouts.

This study supports the addition of a desiccant subsystem to a TAHP for particular climates and favorable gas and electricity rates. First costs per unit of cooling do not increase and energy consumption is significantly reduced.

Future research direction should include integrating component cost relations and a fuel and electricity cost structure into the model to allow optimization on a life-cycle cost or cost-of-service basis; performing sensitivity studies and comparing the effects of component improvements on overall system cost and performance; extending the systems model to allow evaluation of seasonal performance and perform evaluations with climatic data for several typical cities with actual utility rates; and experimentally investigating hybrid cooling system performance to verify system model predictions.

NOMENCLATURE

FLR = fractional load ratio

$T_{\text{cond,in}}$ = condenser air inlet temperature

$T_{\text{evap,in}}^*$ = evaporator air inlet saturation temperature

Greek

ϵ = effectiveness

REFERENCES

- Bharathan, D.; Parsons, J. R.; and Maclaine-cross, I. L. 1987a. Experimental study of an advanced silica gel dehumidifier. SERI/TR-252-2983. Golden, CO: Solar Energy Research Institute.
- Bharathan, D., Parsons, J. R.; and Maclaine-cross, I. L. 1987b. Experimental study of heat and mass exchange in parallel-passage rotary desiccant dehumidifiers for solar cooling applications. SERI/TR-252-2897. Golden, CO: Solar Energy Research Institute.
- Crum, D. R. 1986. "Open cycle desiccant air-conditioning systems." Master's Thesis. Madison, WI: University of Wisconsin.
- Domingo, N. 1986. "Thermally actuated heat pumps with desiccant cooling." Oak Ridge, TN: Oak Ridge National Laboratory.

- Howe, R. R. 1983. "Model and performance characteristics of a commercially sized hybrid air-conditioning system which utilizes a rotary desiccant dehumidifier." Master's Thesis. Madison, WI: University of Wisconsin.
- Jurinak, J. J. 1982. "Open cycle desiccant cooling--component models and systems simulations." Ph.D. Dissertation. Madison, WI: University of Wisconsin, Solar Energy Laboratory.
- Kettleborough, M. R.; Ullah M. R.; and Waugaman, D. G. 1986. "Desiccant cooling systems--a review." Proceedings of the third annual symposium on improving energy efficiency in hot and humid climates. November 18-19, Arlington, TX.
- Maclaine-cross, I. L. 1978. "Comparison of the analogy theory of combined heat and mass transfer in regenerators with a finite difference solution." New South Wales, Australia: University of New South Wales, Department of Mining and Mineral Sciences.
- Maclaine-cross, I. L. 1986. "Brief notes and sample cost calculations on gas engine desiccant hybrid cooling for Australian conditions." New South Wales, Australia: University of New South Wales, School of Mechanical and Industrial Engineering.
- Maclaine-cross, I. L.; and Parsons, J. 1986. A five-ton advanced solid-desiccant solar cooling system with heating and service hot water. SERI/SP-252-2832. Golden, CO: Solar Energy Research Institute.
- Meckler, G. 1986. "Energy-integrated desiccant HVAC system applications." Proceedings of the DOE/SERI desiccant cooling workshop. Chattanooga, TN.
- Meckler, G. 1987. "Solar dehumidification system applications." Proceedings of the ASME/JSME Solar Engineering Conference, pp. 855-865.
- Parsons, B.; Pesaran, A.; Bharathan, D.; and Shelpuk, B. 1987. Analytical study of optimum desiccant dehumidification materials and systems configurations for use with a thermally activated heat pump. Forthcoming. SERI/TR-252-3116. Golden, CO: Solar Energy Research Institute.
- PTY Ltd. 1984. "Rotary heat exchangers." Product Bulletin. Bayswater, Australia: PTY Ltd.
- Schlepp, D. R., and Schultz, K. 1984. Analysis of advanced solar hybrid desiccant cooling systems for buildings. SERI/TR-252-2527. Golden, CO: Solar Energy Research Institute.
- Segaser, C. L. 1977. "Internal combustion piston engines." Integrated community energy systems-technology evaluations. ANL/CES ITE 77-1. Oak Ridge, TN: Oak Ridge National Laboratory.
- Turner, R. H.; Kleiser, J. D.; Chen, R. F.; Domingo, N.; and Chen, F. 1987. "Modeling a thermally activated heat pump with desiccant cooling." ASME WAM. Boston, MA. Paper 87-WA/AES-1.
- Warren, M. L. 1985. "Performance comparison of absorption and desiccant solar cooling systems." Berkeley, CA: Lawrence Berkeley Laboratory.
- Kinast, J. A.; Wurm, J.; Zawacki, T. S.; and Macriss, R. A. 1982. SOLAR-MEC^R development program report. COO-4495-53. Chicago, IL: Institute of Gas Technology.

ACKNOWLEDGMENT

This work was funded by the Conservation and Renewable Energy Division of the U.S. Department of Energy.

TABLE 1
Commercial Equipment Performances

Component	Pressure Drop		
	(in H ₂ O)	(Pa)	
Direct evaporative cooler	0.56	140	$\epsilon = 0.86$
Indirect evaporative cooler	0.56	140	$\epsilon = 0.80$
Air-to-Air Sensible Heat Exchanger	0.16	40	$\epsilon = 0.79$
Air-to-Exhaust Sensible Heat Exchanger	0.16	40	$\epsilon = 0.79$
Air-to-Water Sensible Heat Exchanger	0.20	50	$\epsilon = 0.79$
Other Pressure Drops (ducting, delivery, filters, etc.)	1.00	250	
Dehumidifier	0.60	150	
Vapor Compression Evaporator and Condenser	0.24	60	

ϵ = effectiveness

TABLE 2
Building Load Characteristics

Cooling Load	Ton	kW	
Building Sensible	7.88	27.7	Internal and environmental gains
Latent	2.64	9.3	
Total	10.52	37.0	
Ventilation Sensible	1.31	4.6	Difference between ambient and room for dehumidification airflow
Latent	1.31	4.6	
Total	2.62	9.2	
Total Loads Sensible	9.18	32.3	
Latent	3.95	13.9	
Total	13.13	46.2	

TABLE 3
Comparison of Systems Performance

	System 1	System 2
<u>Performance</u>		
<u>COPs</u>		
Complete System		
Gas	1.42	1.75
Electric	13.77	7.97
Equivalent thermal	1.07	1.01
Vapor Compression Subsystem		
Gas	0.99	1.2
Electric	15.35	*
Equivalent thermal	0.82	*
Desiccant Subsystem		
Gas	11.9	3.3
Electric	11.9	*
Equivalent thermal	2.75	*
<u>Flow Rates</u>		
<u>(kg/s)</u>		
Dehumidifier Supply and Regeneration	0.56	2.47
Vapor Compression Evaporator and Condenser	2.47	2.47
<u>Energy Inputs</u>		
<u>kW</u>		
Internal Combustion Engine (Gas)	30.9	19.5
Auxiliary Regeneration (Gas)	1.3	6.9
Fans (Electric)	3.3	5.8
<u>Hardware Capacities</u>		
<u>kW</u>		
Vapor Compression Subsystem		
Evaporator (all sensible cooling)	30.7	23.4
Condenser (heat rejection)	40.3	39.6
Compressor (work input)	9.6	7.2
Dehumidification Subsystem		
Sensible	1.6	8.9
Latent	13.9	13.9
Total	<u>15.5</u>	<u>22.8</u>
Total Hardware		
Sensible	32.2	32.2
Latent	13.9	13.9
Total	<u>46.2</u>	<u>46.2</u>

*COPs for System 2 are not broken down because of using a single process airstream.

TABLE 4
Dehumidifier Subsystem Operating Specification
(System 1)

Cooling Capacity	4.4 tons (15.5 kW)
Airflow Rate	1000 scfm (0.56 kg/s)
Electrical Power	1.3 kW @120 VAC
Water Consumption	1.56 gph (0.1 L/min) for evaporative cooler
Waste Heat Recovery	46,000 Btu/h (13.5 kW)
Auxiliary Gas Consumption	4400 Btu/h (1.3 kW)
Auxiliary Gas COP*	11.92
Waste Heat Thermal COP**	1.15
Overall Thermal COP***	1.05
Combined Equivalent Thermal COP	2.75
Dehumidifier Wheel Diameter	3.3 ft (1.0 m)

*Based on auxiliary gas input only.

**Including and waste heat input.

***Auxiliary and waste heat input.

TABLE 5
Desiccant Cooling Subsystem Cost
(Nominal 4.4 Ton Capacity)

Component	Estimated Cost (\$)
Desiccant Dehumidifier	460
Counterflow Heat Exchanger	200
Regeneration Heater	150
Direct Evaporative Cooler	165
Dehumidifier, Heat Exchanger Drive Motors and Speed Reducers	70
Fans (2) and Fan Drive Motor	270
Evaporative Cooler Pump	7
Sheet Metal Enclosure	215
Air Filters and Dampers	45
Electronic Controller	50
Miscellaneous Actuators and Mechanical Hardware	<u>60</u>
Assembly Labor	120
Subtotal for Desiccant Subsystem Packaged Unit	1812
Exhaust Heat Recovery Unit (Mounted on Internal Combustion Engine)	<u>350</u>
Estimated Total Manufacturing Cost	2162
\$/Ton of cooling (additional cost/additional capacity)	<u>491</u>

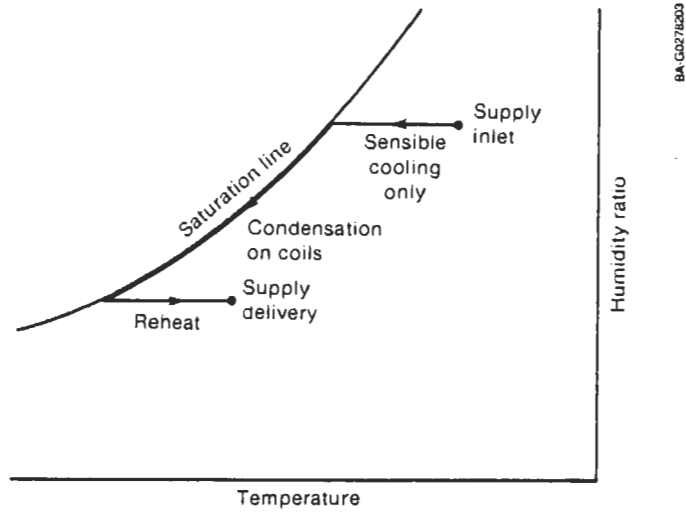


Figure 1. Psychrometric schematic of supply air states in a vapor compression cooling system

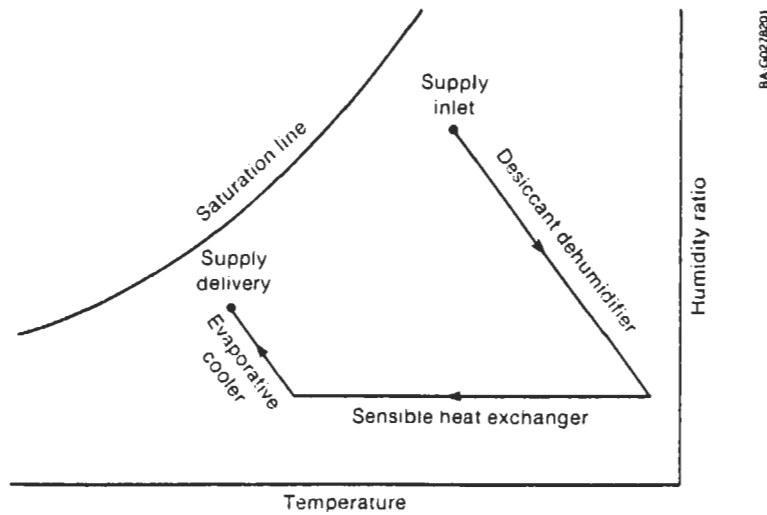


Figure 2. Psychrometric schematic of supply air states in a desiccant cooling system

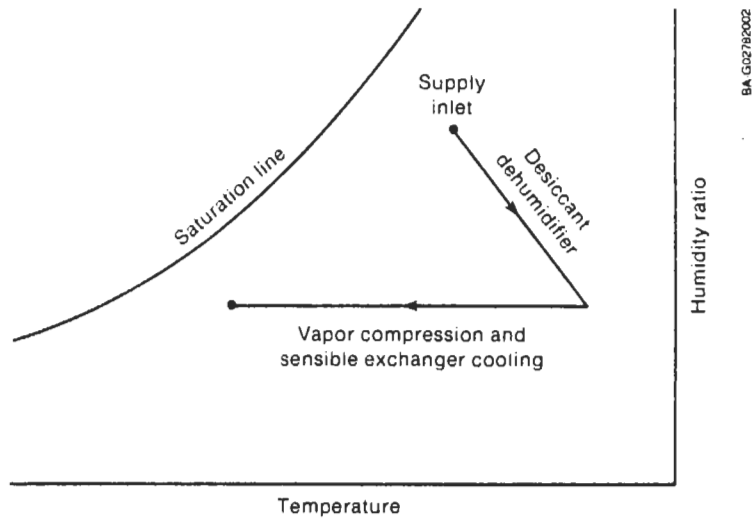


Figure 3. Psychrometric schematic of supply air states in a simple hybrid cooling system

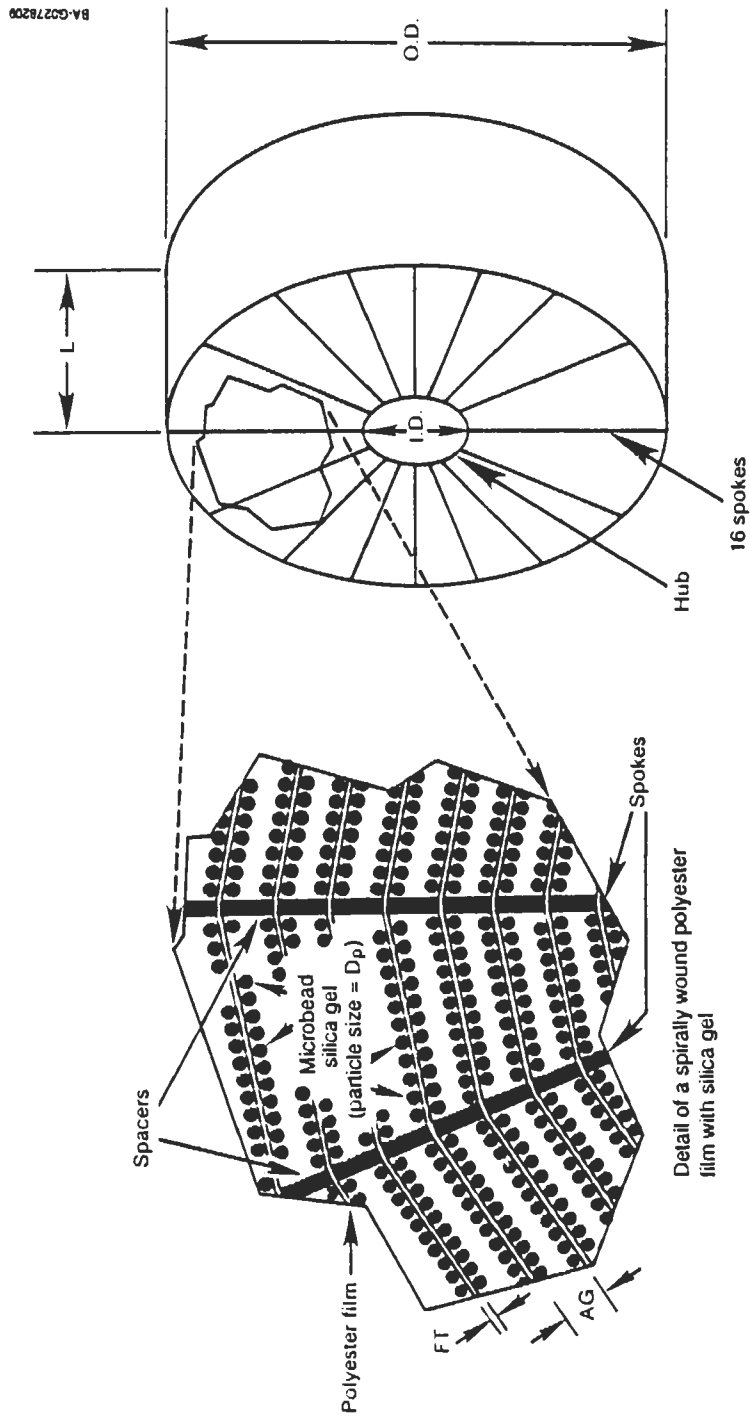


Figure 4a. Schematic of a parallel-plate rotary dehumidifier

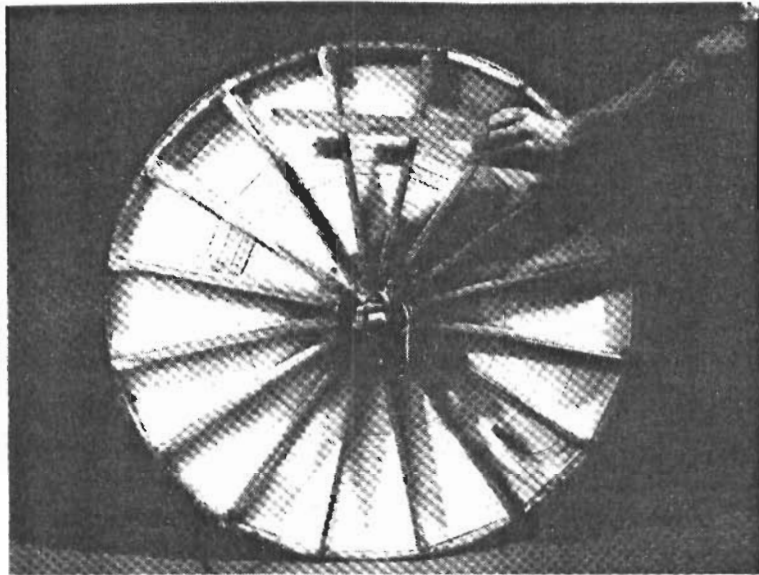


Figure 4b. Front view of Microbead™-silica-gel parallel-plate rotary dehumidifier

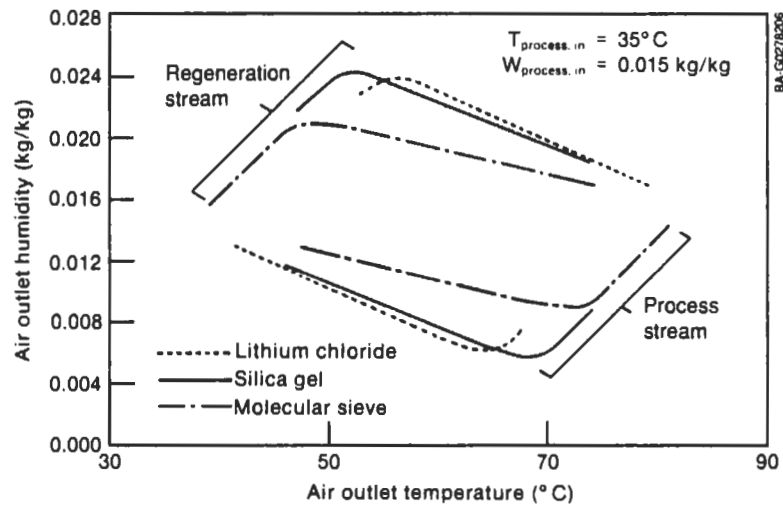
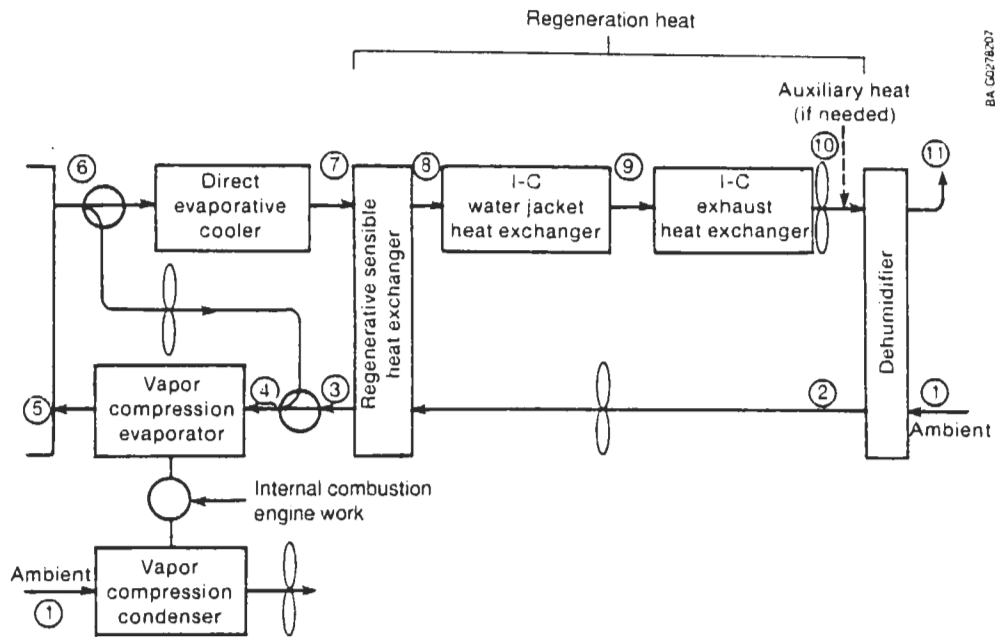
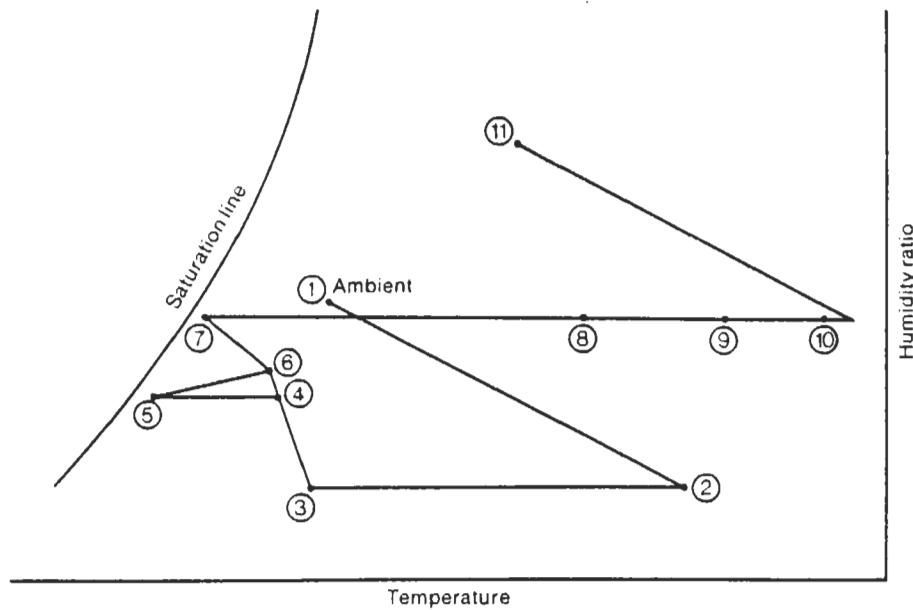


Figure 5. Comparison of wheel performance with airflow rates of 1120 scfm (0.6 kg/s) and an inlet regeneration temperature of 185 F (85°C)

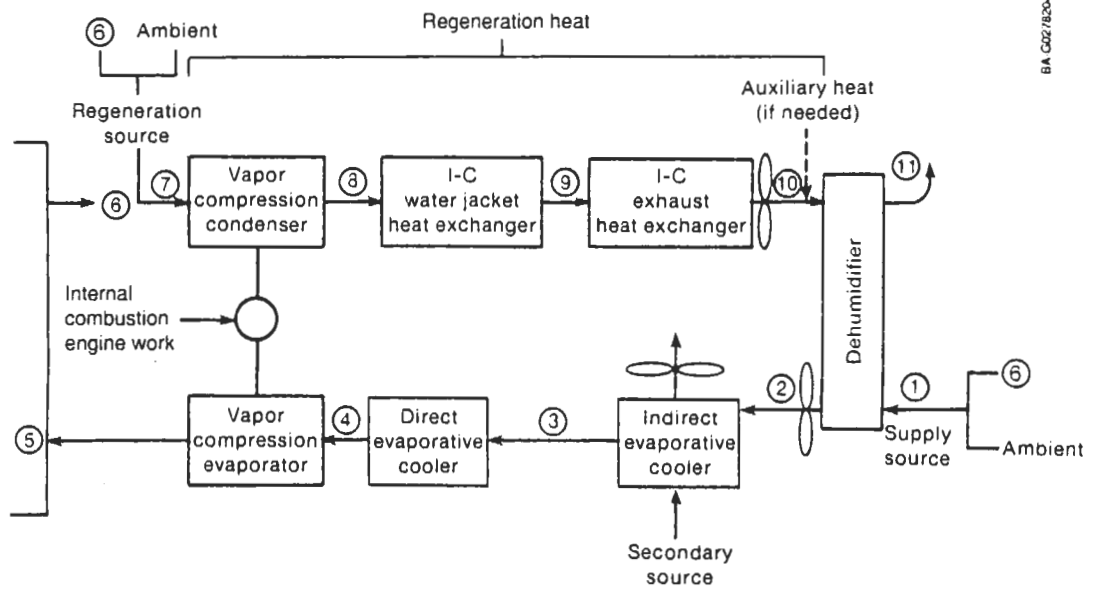


BA G0278207

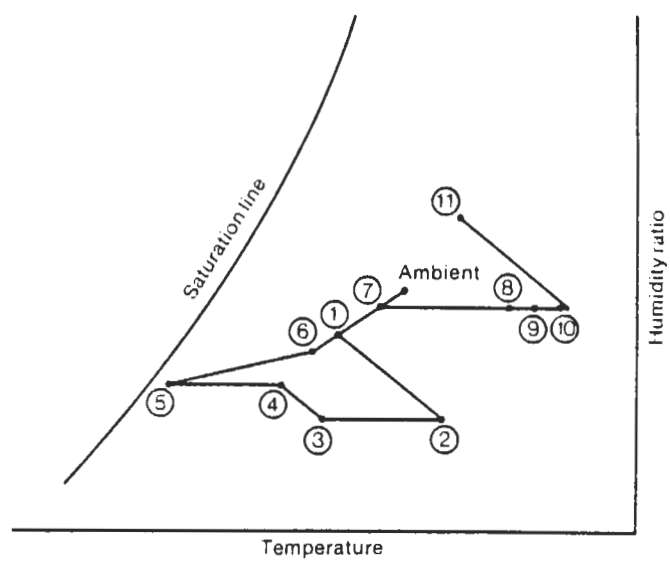


BA G0278206

Figure 6. Schematic and psychrometric chart representation of System 1

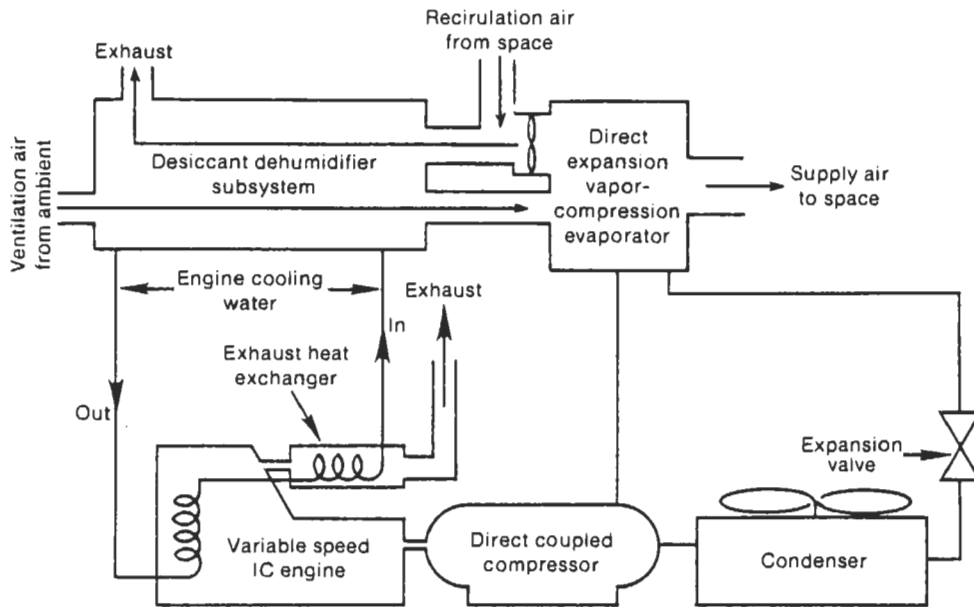


BA G02/8204



BA G02/8205

Figure 7. Schematic and psychrometric chart representation of System 2



BA G02/8211

Figure 8. Integrated system schematic showing subsystem interfaces